REGULAR PAPER

Biomechanical analysis of a new bilateral pedicle screw fixator system based on topological optimization

Li-Xin Guo[1] · **Qing-Dong Wang**[1]

Abstract

Lumbar interbody fusion supplemented with a pedicle screw fixator is an effective treatment for spinal instability, but traditional bilateral pedicle screw fixator may cause some complications, such as degenerative disease of adjacent segments and stress concentration. The purpose of this study is to decrease the stiffness of the rod by using topology optimization to alleviate the above problems. The finite element models of the intact lumbar spine, lumbar spine implanted with traditional bilateral pedicle screw fixator (BPS) and a new fixator designed by using topology optimization (TOD) were developed and compared. Compared with the traditional rigid rod, the volume of TOD rod was reduced by 19.8%. The results showed that the TOD model was similar to the BPS model in terms of the range of motions. TOD reduced intradiscal pressure, stresses in intervertebral discs, and facet contact forces of the adjacent segments. The TOD model significantly decreased the stress concentration region of screws and rods and reduced the stresses in pedicle screws, rods and the junction between the vertebral bodies and screws. TOD fixator may provide a stable condition to the fusion segment as well as the BPS fixator. What's more, TOD alleviates the adjacent segment disease and lower the risk of screw breakage, rod breakage, and vertebral damage. The new rod designed by topology optimization might also be useful in alleviating adjacent segment disease, stress concentration and stress shielding effect.

Keywords Topology optimization · Bilateral pedicle screw fixator · Adjacent segment disease · Stress concentration · Lumbar spine · Finite element analysis

1 Introduction

Spinal fusion surgery is a common treatment for spinal instability. Before this, many scholars have conducted a series of experimental studies and biomechanical analysis of fusion surgery. However, spinal fusion surgery with bilateral pedicle screw fixator (BPS) has several problems, including adjacent segment disease and implant breakage [1–3]. Some clinical reports indicated that spinal fusion might accelerate the degeneration of adjacent segments [4, 5]. These rigid fixators withstood most of the load, which reduced the load shared by the fused segment and produced the stress shielding effect [6]. Strong fixator also changed the load-bearing of intervertebral discs and facets at the adjacent segments and increased range of motion (ROM) and disc pressure at

adjacent segments. It resulted in a series of problems, such as the decrease of bone fusion rate, Osteoporosis, and atrophy of fixed segment, degeneration of adjacent intervertebral discs and facet joints, screw breakage and rod breakage caused by excessive stress concentration [7]. To increase load sharing, many scholars have applied a variety of low stiffness fixators in biomechanical and animal experiments and have achieved encouraging results [8, 9]. However, low stiffness fixators cannot provide spinal stability. Besides, some flexible posterior spinal fixator systems have been developed and put into clinical practice [10]. These implants were designed to restore spinal stability and decreased the load on adjacent segments to reduce the damage to the lumbar spine caused by the fixator system. Some scholars believed that a semi-rigid pedicle screw fixator and a rigid pedicle screw fixator may provide spinal stability, but the former can reduce the stress shielding effect [11]. However, some scholars questioned the spinal stability. Dynesys pedicle screw fixator system was used to treat 50 cases of degenerative lumbar instability. Two years of follow-up showed

✉ Li-Xin Guo
   lxguo@mail.neu.edu.cn

1 School of Mechanical Engineering and Automation, Northeastern University, Shenyang 110819, China

that the reoperation rate of Dynesys system was also high [12].

Meanwhile, Chen et al. used topology optimization to design a new intervertebral cage to allow more bone graft volume to be placed [13]. The disadvantage was that the stress of the new cage was greater than that of the RF cage. The optimization of the implant directly affected the biomechanical properties of the spine. Furthermore, Lin et al. demonstrated the ability of topological optimization to change the biomechanics of the lumbar fusion cages [14]. Topology optimization algorithms generated an optimized material distribution for the set loads and constraints within the given design space [15, 16]. Topology optimization can distribute materials preferably, reduce stress concentration, change stiffness, and achieve different biomechanical behavior by changing the structure. Clinically, some reports have demonstrated that spinal fusion surgery accelerated the degeneration of adjacent segments because of the higher stiffness of rigid rods [4, 5]. The stress concentration caused by the rigid rod caused some problems such as broken screws and broken rods [17]. In this study, the stiffness of the connecting rod was reduced appropriately by reducing the volume of the connecting rod without affecting the lumbar motion, and the overall stiffness of the connecting rod that had been reduced in volume was maximized by adjusting the structure using topology optimization. This study used ABAQUS 6.14 (Dassault Simulia, Providence, USA) to design a new rod and designed to effectively reduce the stiffness of the rod to alleviate the above-mentioned problems. Therefore, the objective of this study is to design a new lumbar spinal fixator by using topology optimization (TOD fixator) to reduce overall stiffness and volume and solve the various problems [6, 18, 19] existing in traditional spinal fixators.

2 Materials and Methods

2.1 Finite Element Modeling and Materials

In this study, a three-dimensional nonlinear L1–L5 finite element model (FEM) of the intact lumbar spine was used. The geometry of the spine was obtained by computer scanning tomographic specimens [20]. The model mainly includes vertebrae, intervertebral discs, endplates, and various ligaments, as shown in Fig. 1. Each vertebral body in L1–L5 is composed of the outer cortical bone and the inner cancellous bone. The cortical bone was C3D8 elements and its thickness is 0.5–1.0 mm. Cancellous bones are tetrahedron elements. Intervertebral disc consists of the annular matrix, annulus fibrosus, and nucleus pulposus. Fibers are crisscrossed in the annular matrix. The Young's modulus of the fiber decreases proportionally from the outer layer to the inner layer. The nucleus pulposus is an incompressible substance. There is a 0.5 mm thick endplate between the vertebral body and the intervertebral disc (Fig. 1). The facet joints were modeled by surf-to-surf. The material properties of lumbar ligament is low elastic. The material properties were assumed to be homogeneous and isotropic [21–23], and the data were adopted from the literature and are given in Table 1.

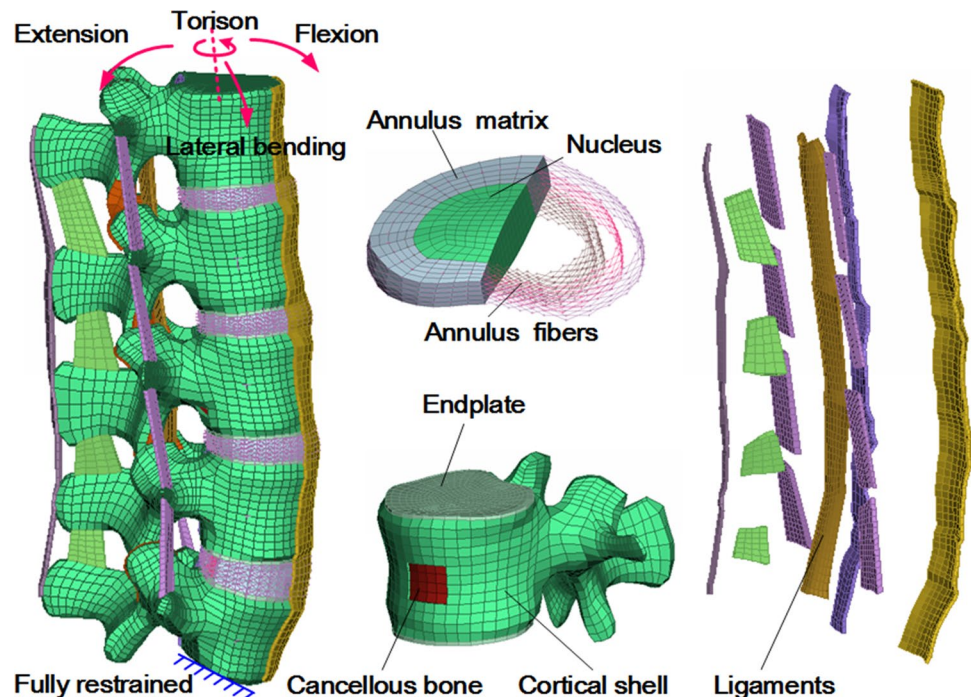**Fig. 1** Finite element model of the intact human L1–L5 lumbar spine

Table 1 Material properties of spinal components

Component	Element type	Young's modulus (MPa)	Poisson's ratio	Cross-sectional area (mm^2)
Bone				
Cancellous bone	C3D4	100	0.2	
Cortical bone	C3D8	12,000	0.3	
Posterior bone	C3D4	3500	0.25	
Endplate	C3D8	500	0.25	
Intervertebral disc				
Nucleus pulposus	C3D8	1	0.49	
Annulus ground substance	C3D8	4.2	0.45	
Annulus fibers	T3D2	357–550	0.3	
Ligaments				
Anterior longitudinal	T3D2	7.8 (<12.0%) 20.0 (>12.0%)		63.7
Posterior longitudinal	T3D2	10.0 (<11.0%) 20.0 (>11.0%)		20
Capsular	T3D2	7.5 (<25.0%) 32.9 (>25.0%)		30
Intertransverse	T3D2	10.0 (<18.0%) 58.7 (>18.0%)		1.8
Interspinous	T3D2	10.0 (<14.0%) 11.6 (>14.0%)		40
Supraspinous	T3D2	8.0 (<20.0%) 15 (>20.0%)		30
Ligamentum flavum	T3D2	15.0 (<6.2%) 19.5 (>6.2%)		40

2.2 The Validation of FEM

In this paper, based on the existing in vitro cadaveric experiments and numerical analysis, the L1–L5 spine finite element model was verified. The present model results are in good agreement with published results, including experimental data and numerical results [24, 25]. The investigations of Renner et al. [24] and Dreischarf et al. [25] presented the compressive deformation, intradiscal pressure, and range of motion of each segment of L1–L5 under follower loads. In summary, the present developed model can be used for further analysis. The detailed model verification results are shown in Table 2.

2.3 New Lumbar Spinal Fixator by Using Topology Optimization

Topology optimization theory is to satisfy the objective function as far as possible under constraint conditions. Structural energy is used to measure the stiffness of the rod, and minimizing the structural energy is equivalent to maximizing overall structural stiffness [13]. In this paper, topology optimization is to minimize the structural energy of the rod, and its structural volume (V) is the constraint.

$$C(a) = EA/l, \ (N/mm) \tag{1}$$

$$C(b) = 3EI/l^2, (N/mm) \tag{2}$$

where l the length, A the area, E Yong's modulus, I the second moment of area, C(a) the axial stiffness of rod, C(b) the bending stiffness. Based on the above formula, the volume or parameters of the connecting rod directly affect its stiffness [26, 27]. Therefore, the reduction in the stiffness of the connecting rod is determined by the decrease in its volume (the constraint), and topology optimization is to maximize the structural rigidity of the rod that has been reduced in volume by adjusting the structure. Appropriate reduction of the rod volume (the constraint) determines that the stiffness of the rod can be decreased and ensures that the lumbar motion cannot be affected. Some numerical studies indicated that the stiffness of the connecting rod greater than 1000 N/mm had only a minor effect on intersegmental rotation [28, 29]. An in-vitro Biomechanical Study by Kwonsoo et al. investigated the effect of the connecting rod ($\Phi 5.5 \times L42.5$ mm) stiffness on the motion of the lumbar spine instrumented with pedicle screw fixator at L4–L5 level. They found that the range of motion was only marginally increased when the implant stiffness beyond 70 GPa (aluminum) [30]. Since the bending stiffness of rod directly affects the stability of the diseased lumbar spine and its axial stiffness is much larger than the bending stiffness, many studies and present research have focused on the bending stiffness of the rod. In the present study, based on the parameters of rod, the change of the connecting rod stiffness between 5220 and 8947 N/mm may marginally affect the range of motion of the lumbar spine. To ensure the stability between the screws and the connecting rod, only the area about 16.5 mm in the middle of the rod was reduced, as Fig. 3 shown. Based on the formula of

Table 2 Comparison of the results for the present study with the experimental data of Renner et al. [24] and numerical results of Dreischarf et al. [25] under static loading conditions

Loading condition	Chosen parameters	Spinal levels			
		L1–L2	L2–L3	L3–L4	L4–L5
1200 N FL					
Renner et al.	Compression (mm)	1.20 ± 0.30	1.50 ± 0.80	1.50 ± 0.50	1.60 ± 0.50
Present study	Compression (mm)	1.48	1.59	1.83	1.71
+8/-6 Nm FXT-EXT with 800 N FL					
Renner et al.	Segmental ROM (deg)	5.7 ± 2.7	6.4 ± 1.5	8.30 ± 2.1	10.0 ± 2.8
Present study	Segmental ROM (deg)	5.26	5.5	6.36	7.45
± 6 Nm left–right LAT					
Renner et al.	Segmental ROM (deg)	10.5 ± 5.6	12.3 ± 6.7	8.4 ± 2.9	10.0 ± 3.0
Present study	Segmental ROM (deg)	5.81	6.74	5.87	7.54
7.5 Nm FXT with 1175 N FL					
Dreischarf et al.	Intradiscal pressure (MPa)	1.8 ± 0.1	1.5 ± 0.4	1.3 ± 0.3	1.3 ± 0.3
Present study	Intradiscal pressure (MPa)	1.87	1.78	1.58	1.5
7.5 Nm EXT with 500 N FL					
Dreischarf et al.	Intradiscal pressure (MPa)	0.6 ± 0.4	0.5 ± 0.3	0.5 ± 0.4	0.5 ± 0.4
Present study	Intradiscal pressure (MPa)	0.46	0.61	0.66	0.64
7.8 Nm LAT with 700 N FL					
Dreischarf et al.	Intradiscal pressure (MPa)	0.7 ± 0.3	0.7 ± 0.4	0.6 ± 0.3	0.6 ± 0.4
Present study	Intradiscal pressure (MPa)	0.55	1.05	0.9	0.79

FLX, flexion; EXT, extension; LAT, lateral bending; FL, follower load; ROM, range of motion

calculating the bending stiffness of the rod (2), when the volume of the middle area of the rod was reduced by 50%, the maximum stiffness of rod was approximately 7582 N/mm which may not affect the range of motion of the lumbar spine. Therefore, the process was expected to reduce the volume of the area approximately 16.5 mm in the middle of the rod by 50% and iterate 30 times. Convergence tolerance is defined as 0.0001.

Topology optimization is as follows: objective function: minimize U_c, U_c: the energy of structural compliance; limitation: $0 < \eta_i < 1$ (i = 1,2,3,…,n), η_i: the internal pseudo-densities that are assigned to each element (i) in the topology

$$V = \sum_{i}^{n} \eta_i V_i \tag{3}$$

$$V \leq V_0 V^* \tag{4}$$

$$E_i = E(\eta_i) \tag{5}$$

$$\{\sigma_i\} = [E_i]\{\varepsilon_i\} \tag{6}$$

V: the computed volume, V_0: the original volume, V^*: the amount of material to be removed, V_i: the volume of element (i), E_i: the elasticity tensor for each element, E: the elasticity tensor, σ_i: the stress vector of element (i), ε_i: the strain vector of element (i).

The density variable, η_i varied between 0 and 1, where η_i near 1 represents the material to be retained, while η_i close to 0 represents the material that should be removed. (Fig. 2a) Topology optimization was carried out in flexion, extension, lateral bending, and torsion. Then, the new rod structure deriving from topology optimization was called the topological rod (Fig. 2b). Compared to the rigid rod ($\Phi 5.5 \times L42.5$), the volume of the topology rod was reduced by approximately 19.8%. From the results of topology optimization, the effective materials were located on anterior–posterior and outside direction of the rod. Therefore, the invalid material located inside was removed, that is, the topology optimization of the connecting rod. Based on our calculation, the safety factor of the new connecting rod is sufficient to meet the actual engineering needs.

2.4 FEM of the Traditional BPS Fixator and New TOD Fixator

The BPS and TOD fixators were bilaterally implanted into the L4–L5 vertebral body finite element model [31, 32]. The reason for the L4–L5 level is that the prevalence of L4–L5 in individuals suffering from lumbar diseases is greater than other intervertebral discs [33, 34]. The traditional bilateral pedicle screw fixator system includes pedicle screws ($\Phi 6 \times L55$ mm) and longitudinal rods ($\Phi 5.5 \times L42.5$ mm) (Fig. 3a) [35]. Titanium (E = 120,000 MPa, v = 0.3) material properties were defined for pedicle screws and longitudinal rods. The TOD

Fig. 2 a The rigid rod in the L4–L5 motion segment, the arrow indicates the location of redundant material in inside aspect of spinal model, **b** the new design (topology rod) and the size of the topology rod
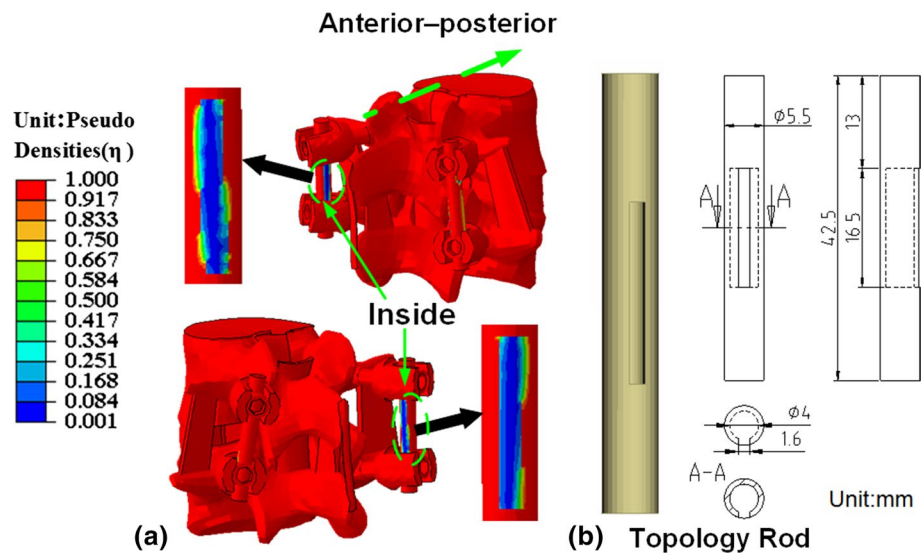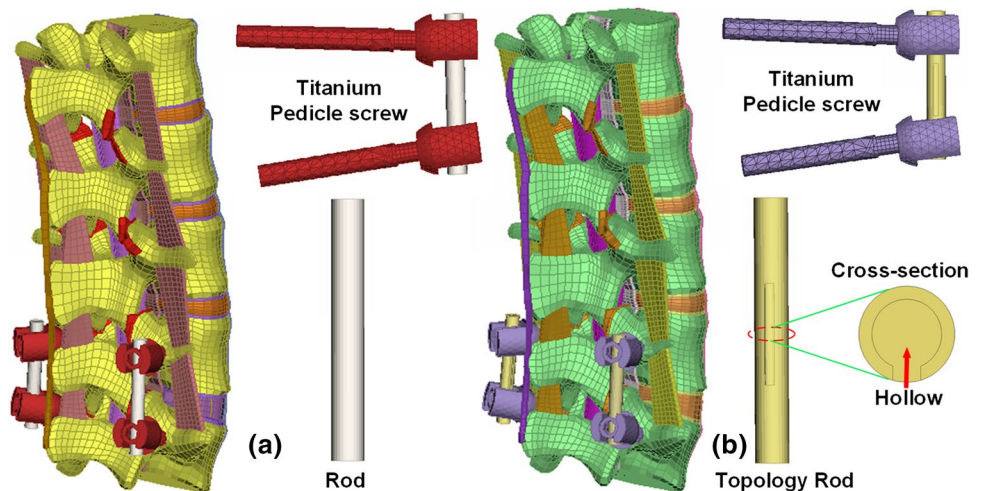

Fig. 3 (a) The finite element model of L1–L5 fusion spine with BPS fixator (b) The finite element model of L1–L5 fusion spine with TOD fixator

fixator system includes pedicle screws and rods designed by topology optimization ($\Phi 5.5 \times \Phi 4 \times L42.5$ mm) (Fig. 3b). Cage (L16 × W10 × H8 mm) provided support stability for intervertebral fusion. PEEK (E = 3600 MPa, v = 0.3) material properties were defined for the cage. This study adopted the single cage method [36], one of the commonly used fusion methods, to improve the stability of the lumbar spine.

In this paper, the model of pedicle screw was simplified and structures such as threads and chamfers that have little effect on mechanical properties were removed. To implant the cage and pedicle screw, one of the facet joints between L4 and L5 vertebral bodies was removed. Moreover, the intact lumbar spine model (Intact) was created to compare with the BPS model and the TOD model.

2.5 Loading and Boundary Conditions

The constraint type 'Tie' was defined between pedicle screws and vertebral bodies, as well as pedicle screws and longitudinal rods. To simulate the condition after fusion, the interfaces between cage and endplates were bonded via node sharing. The lower surface of the L5 vertebral body was fixed throughout the simulation process. The nodes on the upper surface of L1 were combined with reference points for load application. A preload of 150 N was applied to the superior surface of the L1 level [28]. The nodes on the uppermost surface of the L1 vertebra were coupled to a reference node for load application. A 10Nm moment was applied to this reference node. And

the flexion, extension, torsion, and lateral bending of the model were achieved by changing the direction of torque.

3 Results

The numerical results about adjacent segment disease and stress concentration such as the disc stress, intradiscal pressure, and Von-Mises stress distributions of rod and pedicle screw were compared and listed. Essential indexes such as range of motion and stiffness of the spine were used to assess the stability of the structure and stable environment for the fused vertebrae. The Von-Mises stress distributions of the vertebrae with TOD fixator and BPS fixator under the different loads were compared and analyzed. The stress in L4/5 endplates was used to assess the load sharing of the TOD and BPS model.

3.1 Range of Motions

The ROMs of the fusion lumbar segment (L4–L5) in the TOD and BPS models were all under 1.06º and were reduced in all motions when compared to Intact. For the fused segment (L4–L5) level, the ROMs of TOD were similar to those of BPS. For example, in all motions, the ROMs of L4/5 were 0.65, 1.05, 0.68, and 0.87 degrees for TOD, and 0.57, 1.06, 0.52, and 0.88 degrees for BPS. For the adjacent segments (L1–L2, L2–L3, and L3–L4), the TOD model generated smaller ROMs in all motions compared with the BPS model. The stiffness of the BPS and TOD were, at

most, 1.83 and 2 times the stiffness of the intact model in all motions (Table 3).

3.2 Stress in Intervertebral Discs and Facet Contact Forces

It was found in Fig. 4a, b that the stress of the L2/3 and L3/4 discs in the TOD model were smaller than those of the BPS model in all motions. Especially in torsion, the stresses of the L2/3 and L3/4 disc were 0.212, 0.236 MPa for the TOD model, and 0.458, 0.469 MPa for the BPS model. The TOD model decreased the intradiscal pressure of L2/3 and L3/4 discs in all motions compared with the BPS model.

As illustrated in Fig. 5a, b that the facet contact force between L2 and L3 in the TOD model were smaller than the BPS model in extension, torsion, and lateral bending. For example, the L2/3 facet contact forces were 32.9, 156, and 44.4 N in extension, torsion, and lateral bending for TOD, and 52.8, 204, and 52.6 N for BPS. The force between L3 and L4 of TOD in extension and torsion (196 and 223 N) decreased the facet contact force compared to the BPS model (205 and 203 N). The TOD model increased the Von-Mises stress of L4/5 endplates compared to the BPS model (Fig. 5c, d). Especially in flexion, the stresses of the L4 inferior and L5 superior discs were 0.37 (119%), 0.361 (118%) MPa for the TOD model, and 0.312 (100%), 0.305 (100%) MPa for the BPS model. This implied that the contact stress of TOD model at the fusion level increased by 18% compared with the BPS model, and this might also improve the stress shielding effect.

Table 3 ROMs and stiffness comparison for each motion segment in the three FE models

	ROMs(degree)				Total lumbar ROMs (degree)	Stiffness (Nm/degree)
	L1/L2	L2/L3	L3/L4	L4/L5		
Flexion						
Intact	6.2	3.79 (100%)	1.85 (100%)	2.53 (100%)	14.40	0.69 (100%)
TOD	3.99	2.86 (75.5%)	1.48 (80.0%)	0.65 (25.7%)	8.98	1.11 (161%)
BPS	4.23	3.16 (83.4%)	1.63 (88.1%)	0.57 (22.5%)	9.6	1.04 (151%)
Extension						
Intact	6.54	7.53 (100%)	5.06 (100%)	6.72 (100%)	25.85	0.39 (100%)
TOD	4.70	6.49 (86.2%)	5.00 (98.8%)	1.05 (15.6%)	17.20	0.58 (149%)
BPS	4.92	6.83 (90.7%)	5.21 (131%)	1.06 (15.8%)	18.01	0.56 (143%)
Torsion						
Intact	2.6	1.53 (100%)	1.34 (100%)	1.04 (100%)	6.52	1.53 (100%)
TOD	2.52	1.69 (110%)	1.10 (82.1%)	0.68 (65.4%)	5.99	1.70 (111%)
BPS	2.52	2.24 (146%)	1.61 (120%)	0.52 (50.0%)	6.89	1.45 (94.8%)
Lateral bending						
Intact	5.82	6.74 (100%)	5.88 (100%)	6.04 (100%)	24.47	0.41 (100%)
TOD	3.01	4.48 (66.5%)	3.77 (64.1%)	0.87 (14.4%)	12.13	0.82 (200%)
BPS	3.29	4.97 (73.7%)	4.25 (72.3%)	0.88 (14.6%)	13.39	0.75 (183%)

The parentheses indicate the following value: $\frac{\text{Intact, TOD, or BPS}}{\text{Intact}} \times 100\%$

Fig. 4 Stress in intervertebral discs and intradiscal pressure of the L2/3 and L3/4 levels for the three FE models
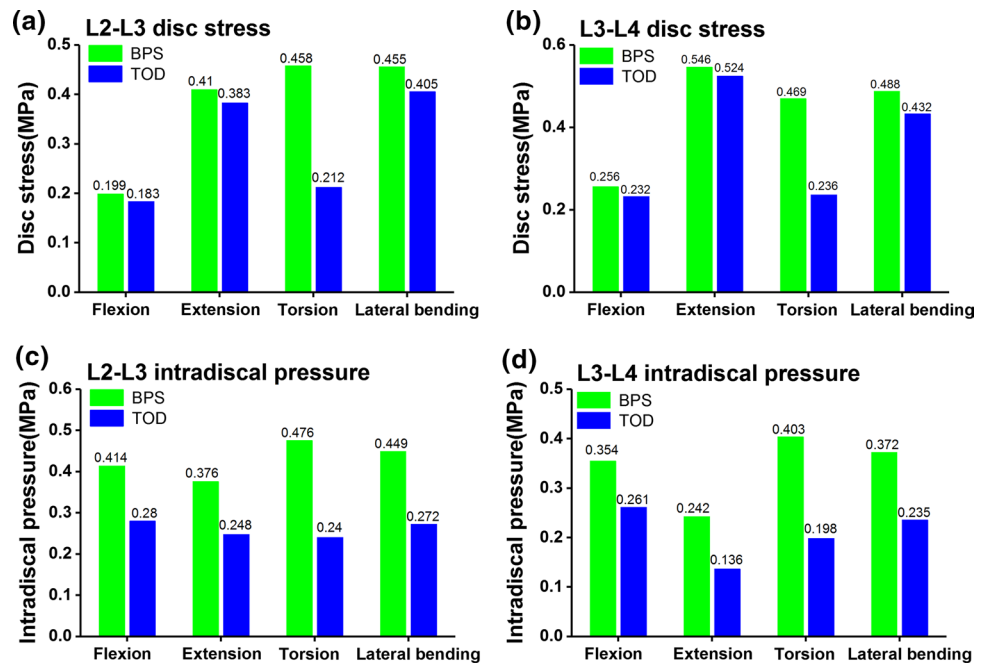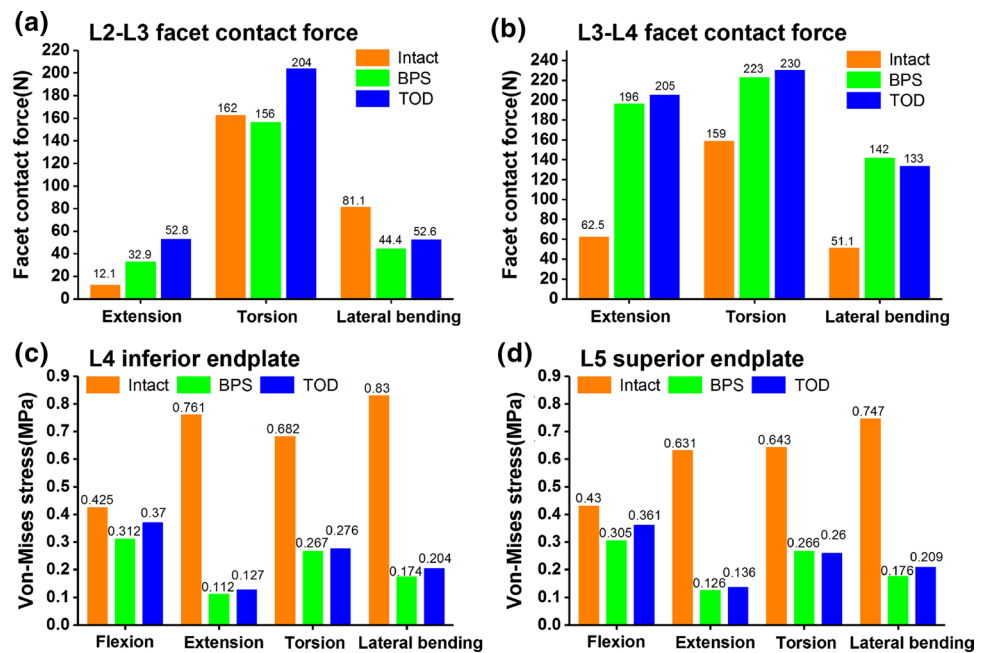

Fig. 5 Facet contact forces of the L2/3 and L3/4 levels and stress in L4/5 endplates for the three FE models

3.3 Stress in Pedicle Screws and Rods

It was found in Fig. 6 that the stress was concentrated at the neck of the pedicle screw for TOD and BPS models in all motions. In flexion, extension, torsion, and lateral bending, the pedicle screw of TOD exhibited smaller stress than it did in BPS (Fig. 6). The max stresses of screws in TOD were 52%, 64.8%, and 79.3% of those of BPS in flexion, torsion, and lateral bending, respectively. What's more, in torsion, the TOD model decreased the high-stress region in screws relative to the same region in the BPS model (Fig. 6). It was observed in Fig. 7 that the stress concentration region was located in the middle of the rod in all motions, and TOD decreased the stress concentration region of rods compared to BPS. Moreover, TOD reduced the maximum stresses of the rod in flexion, extension, torsion, and lateral bending compared to those of BPS, and the difference, at most, can be up to 50.3% in torsion.
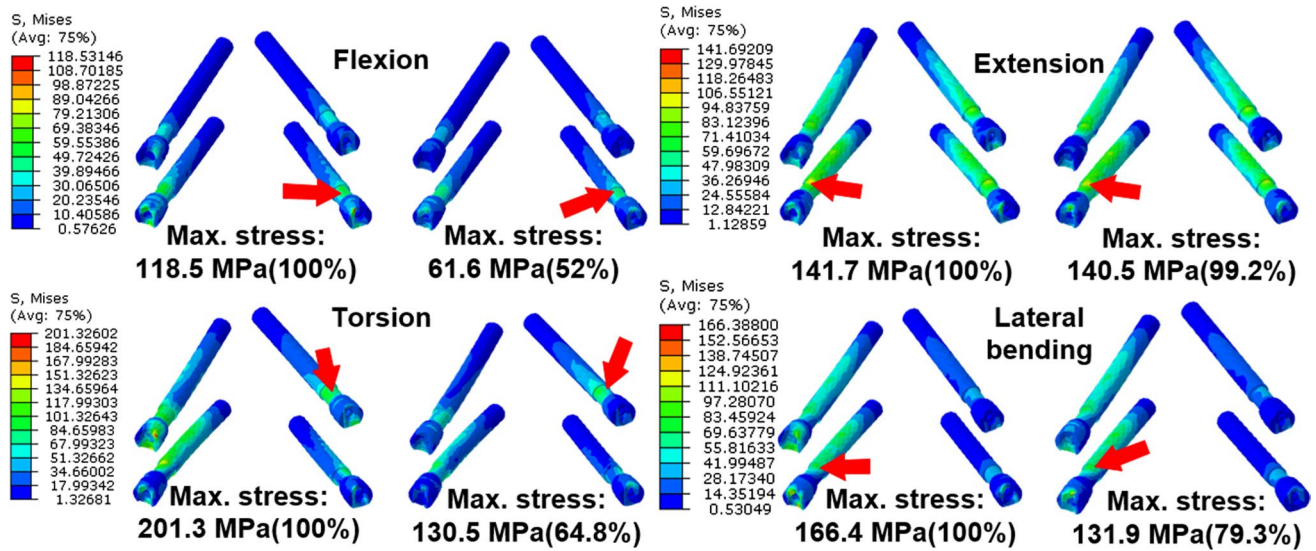
Fig. 6 Screw stress distribution in pedicle screws for all motions. The arrowhead indicates the position of maximum stress (left: BPS system, right: TOD system)
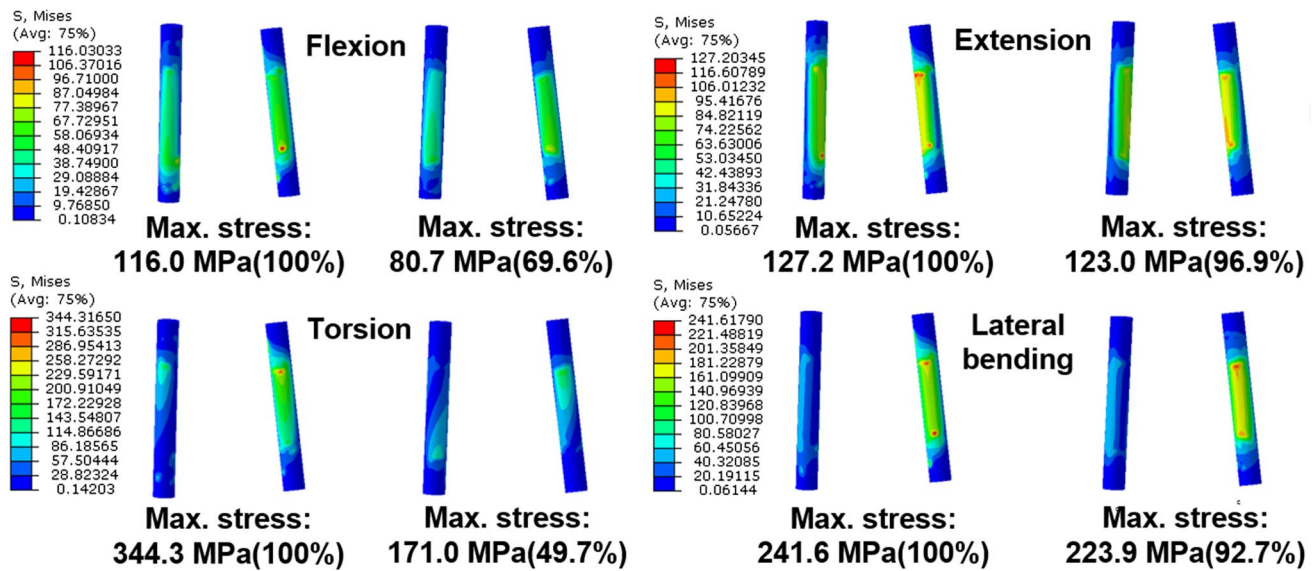

Fig. 7 Screw stress distribution in rods for all motions (left: BPS system, right: TOD system)

3.4 Stress in L4 and L5 Vertebra Body

In order to better illustrate the impact of the pedicle screw on the L4 and L5 vertebral bodies, the positions of four screws were marked as position1 (upper left), position2 (lower left), position3 (upper right), and position4 (lower right), in Fig. 8, and the stresses of the position 1,2,3,4 in BPS were compared with the stresses of same positions in TOD, respectively. The stress concentrations of the L4–L5 vertebral body in BPS and TOD were mainly located at the junction between screws and the vertebral bodies, as shown in Figs. 8 and 9 (Positions 1,

2, 3, and 4). The stresses of the position1, 2, 3, and 4 in TOD were smaller than the stresses of the same position in BPS in all motions. And in torsion, the stresses of the position1, 3 in BPS were 2.03 and 1.39 times of those in TOD (Fig. 9).

4 Discussion

At present, the rigid traditional bilateral pedicle screw lumbar fixator bears most of the load, which is prone to lead to degenerative disc and facet joint disease at the adjacent
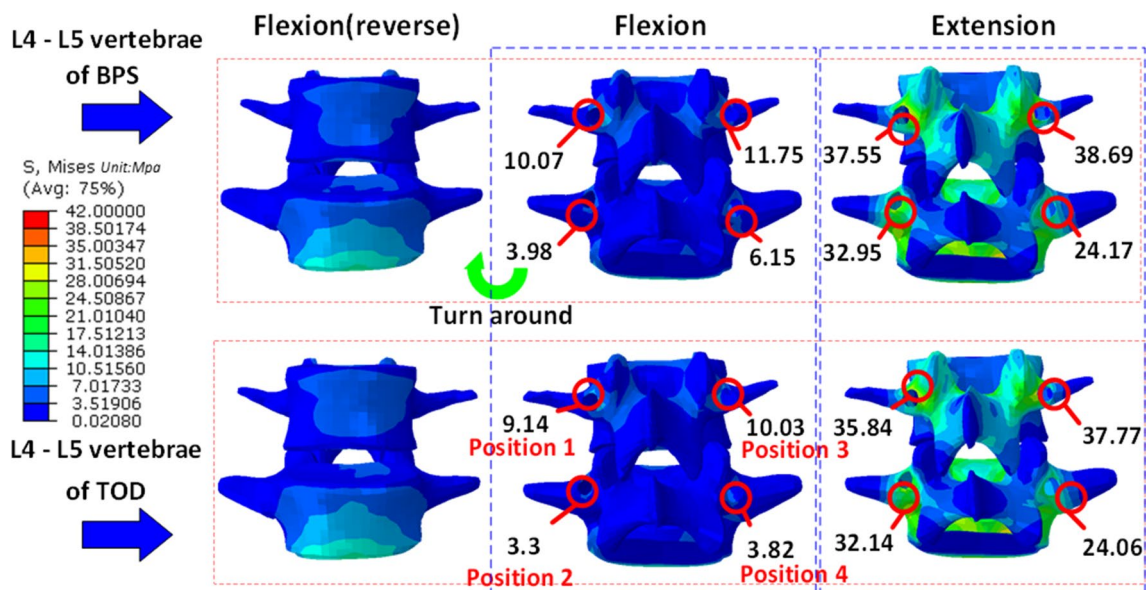
Fig. 8 The von-Mises stress distribution of the L4–L5 of TOD and BPS vertebrae in flexion and extension
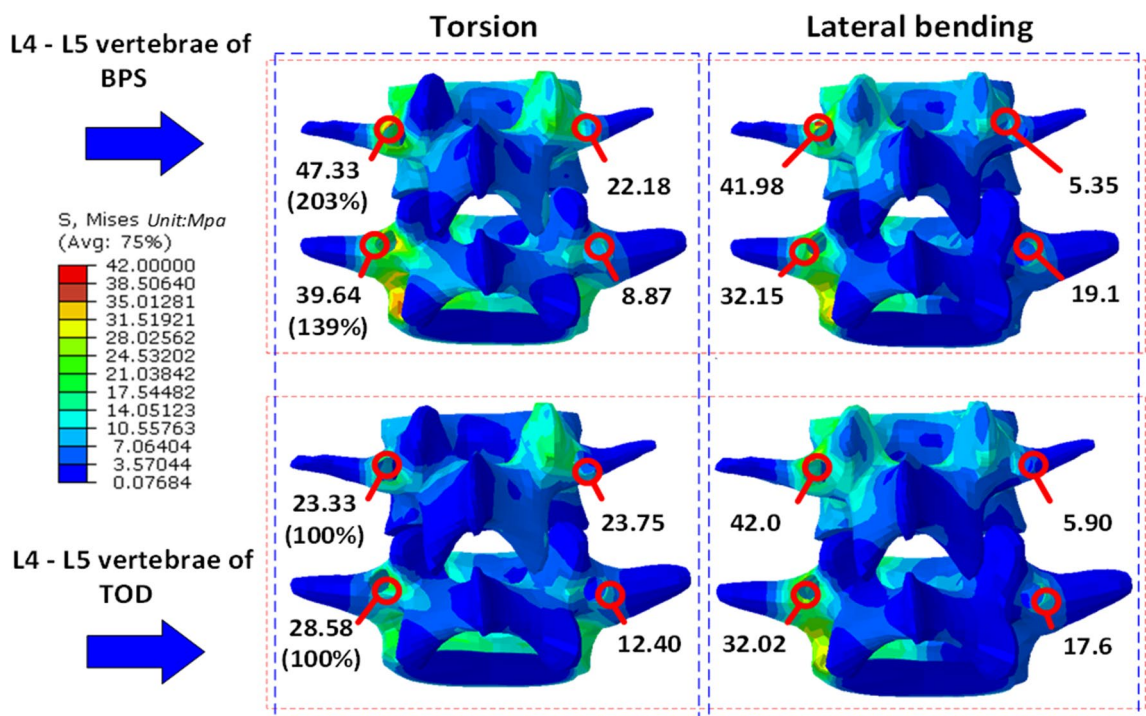

Fig. 9 The von-Mises stress distribution of the L4–L5 vertebrae of TOD and BPS in torsion and lateral bending

segments. At the same time, excessive concentration of stress may lead to problems such as broken rods and broken screws. To solve these problems, all kinds of new fixators came into being, but there were many problems. In this paper, a new lumbar fixator was designed by topology optimization to alleviate the above problems. Compared to the

rigid rod, the volume of the topology rod was reduced by approximately 19.8%. The new lumbar fixator saved material and avoided damaging the tissue around the spine to a greater extent.

ROMs and facet contact forces were the main indexes to evaluate the performance of the fusion spine. Freudiger

et al. found that the BPS model reduced ROMs compared to the intact spine in flexion, extension, and lateral bending [37]. Our results agree with previous studies including experiments and biomechanical analysis. The ROMs of the TOD model were similar to the BPS model. As far as ROMs are concerned, the ability of the TOD model is obviously not losing to the BPS model. In terms of the facet contact force, the performance of the BPS model was consistent with the result of Rohlmann et al.'s study [38]. They found that the bilateral pedicle screw fixator system increased facet joint forces at other levels for axial rotation and extension. In this paper, the results about the facet contact force showed that the new topology-optimized lumbar fixator significantly reduced the facet contact forces at adjacent segments, thereby reducing the possibility of degenerative lesions. Judging from previous tests and finite element analysis results, the stresses of the discs at adjacent segment increased when BPS was used, and our result was consistent with the earlier experimental and numerical results that the stress on disc and facet joints of the adjacent segments increased after implanting the pedicle screw fixator [39, 40]. The stresses and intradiscal pressures in the L2/3 and L3/4 disc (the adjacent segments) of the TOD model were less than those of the BPS model in all motions, especially in torsion. Based on our results, we believe that the new fixator may reduce the risk of adjacent segment disease and degenerative lesions caused by traditional BPS fixator. The TOD model increased the stress in the fused endplates (L4 inferior and L5 superior endplates) compared with the BPS model, especially in flexion. This implies that the new fixator increase the load sharing of the vertebrae and reduce the stress shielding effect compared with the traditional bilateral pedicle screw fixator. The traditional BPS fixator may provide stability for the fixed segment, but the rigid fixator led to stress concentration and led to broken screws and rods [7, 41, 42]. In this study, the stress concentration regions in rods and pedicle screws of TOD and BPS were in the middle of rods and the neck of the pedicle screws. And some researches predicted the same trend about the stress concentration region in rods and pedicle screws [43, 44]. The pedicle screws and rods in TOD exhibited smaller stress than it did in BPS in all motions. Especially in flexion and torsion, the maximum stresses in screws and rods of TOD reduced to half of screws and rods in BPS. The properties of the pedicle screw and vertebral cortical bone were different, and the pedicle screw may directly damage the vertebral cortical bone [45]. The stresses in the junction between pedicle screws and vertebral bodies are usually larger, so the vertebral bodies tend to be damaged easily. In this paper, the stress concentration regions in vertebral bodies of BPS and TOD were all located at the junction between screws and vertebral bodies. This result was consistent with the study of Chen et al. that the peak stress of vertebrae was located

at the junction of the screw and bone, which was consistent with the location of bone fracture observed in a clinical setting [46]. The maximum stresses in vertebral bodies of the TOD model were similar to those of BPS in flexion, extension, and lateral bending. But in torsion, the maximum stress in the vertebral bodies of TOD decreased obviously compared with the BPS model. Therefore, we infer that the new instrumentation may decrease the likelihood of rod breakage, screw breakage, and vertebral injury compared to the traditional BPS fixator.

The potential limitations in this study are as follows. The linear simplification or piecewise linear simplification used in this study for the material property of spinal ligaments and intervertebral discs with non-linear behaviors might influence the accuracy of calculation results. The spinal ligaments and intervertebral discs show obvious nonlinearity, such as viscoelastic, poroelastic, degenerative, etc. In fact, in many finite element analyses [47], the linear simplification of material property of human spine tissues was still adopted. This simplification did not make a high influence on the accuracy of calculation results if choosing appropriate linear material parameters. And the fact that our results were consistent with the in vitro experiments confirms the reality of our spine FE model. The threads and the chamfer on the screws and cage were simplified. The small impact of the threads and chamfer was not enough to affect the overall results.

5 Conclusions

In this study, the topology optimization method was used to optimize the connecting rod, and a new lumbar fixator was designed to solve the problems of traditional bilateral lumbar fixator, such as the degenerative disease of the adjacent segments and stress concentration. The results of biomechanical finite element analysis showed that compared with the traditional fixator, the new fixator may reduce intradiscal pressure, the stresses of adjacent intervertebral discs, and the facet contact forces, thus reducing adjacent segment disease, degenerative lesions, and the stress shielding effect. What's more, the new lumbar fixator may decrease stress concentration and reduce the likelihood of rod breakage, screw breakage, and vertebral injury. The topological rods in this study are less volume, more economical, and avoid damage to vertebral tissue. The present study may provide useful information for alleviating adjacent segment disease and stress concentration of the fixator in lumbar interbody fusion.

Compliance with Ethical Standards

Conflict of interest They authors declare that they have no conflict of interest.

Ethical Approval Not required.

References

1. Erbulut, D. U., Zafarparandeh, I., Ozer, A. F., & Goel, V. K. (2013). Biomechanics of posterior dynamic stabilization systems. *Advances in Orthopedics, 2013*, 1–6.

2. Fan, W., & Guo, L. X. (2018). Biomechanical comparison of nucleotomy with lumbar spine fusion versus nucleotomy alone: Vibration analysis of the adjacent spinal segments. *International Journal of Precision Engineering and Manufacturing, 19*(10), 1561–1568.

3. Gibson, J. N., Grant, I. C., & Waddel, G. (1999). The Cochrane review of surgery for lumbar disc prolapse and degenerative lumbar spondylosis. *Spine, 24*(17), 1820–1832.

4. Choi, H. W., Kim, Y. E., & Chae, S. W. (2016). Effects of the level of mono-segmental dynamic stabilization on the whole lumbar spine. *International Journal of Precision Engineering and Manufacturing, 17*(5), 603–611.

5. Schlegel, J. D., Smith, J. A., & Schleusener, R. L. (1996). Lumbar motion segment pathology adjacent to thoracolumbar, lumbar, and lumbosacral fusions. *Spine, 21*(8), 970–981.

6. Chang, C. L., Chen, C. S., Huang, C. H., & Hsu, M. L. (2012). Finite element analysis of the dental implant using a topology optimization method. *Medical Engineering & Physics, 34*(7), 999–1008.

7. Stančić, M. F., Mićović, V., & Potočnjak, M. (2000). Hook-rod with pedicle screw fixation for unstable spinal fracture–technical note. *Journal of Neurosurgery, 92*(1), 117–121.

8. Kang, K. T., Kim, H. J., Son, J., Yeom, J. S., & Chun, H. J. (2015). Comparing an instrumented posterior fixation system with rigid and semi-flexible rods using finite element analysis. *International Journal of Precision Engineering and Manufacturing, 16*(1), 163–170.

9. Oda, I., Abumi, K., Yu, B. S., Sudo, H., & Minami, A. (2003). Types of spinal instability that require interbody support in posterior lumbar reconstruction: An in vitro biomechanical investigation. *Spine, 28*(14), 1573–1580.

10. Korovessis, P., Papazisis, Z., Koureas, G., & Lambiris, E. (2004). Rigid, semirigid versus dynamic instrumentation for degenerative lumbar spinal stenosis: A correlative radiological and clinical analysis of short-term results. *Spine, 29*(7), 735–742.

11. Stancić, M. F., Gregorović, E., Nozica, E., & Penezić, L. (2001). Anterior decompression and fixation versus posterior reposition and semirigid fixation in the treatment of unstable burst thoracolumbar fracture: Prospective clinical trial. *Croatian Medical Journal, 42*(1), 49–53.

12. Grob, D., Benini, A., Junge, A., & Mannion, A. F. (2005). Clinical experience with the dynesys semirigid fixation system for the lumbar spine: Surgical and patient-oriented outcome in 50 cases after an average of 2 years. *Spine, 30*(3), 324–331.

13. Zhong, Z. C., Wei, S. H., Wang, J. P., Feng, C. K., Chen, C. S., & Yu, C. H. (2006). Finite element analysis of the lumbar spine with a new cage using a topology optimization method. *Medical Engineering and Physics, 1*, 90–98.

14. Lin, C. Y., & Lamarca, W. F. (2010). Structural and mechanical evaluations of a topology optimized titanium interbody fusion cage fabricated by selective laser melting process. *Journal of Biomedical Materials Research Part A, 83A*(2), 272–279.

15. Bendsoe, M. P., & Kikuchi, N. (1988). Generating optimal topologies in structural design using a homogenization method. *Computer Methods in Applied Mechanics & Engineering, 71*(2), 197–224.

16. Guo, L. X., & Yin, J. Y. (2019). Finite element analysis and design of an interspinous device using topology optimization. *Medical and Biological Engineering and Computing, 57*(1), 89–98.

17. Galbusera, F., Bellini, C. M., Anasetti, F., Ciavarro, C., Lovi, A., & Brayda-Bruno, M. (2011). Rigid and flexible spinal stabilization devices: A biomechanical comparison. *Medical Engineering and Physics, 33*(4), 490–496.

18. Kim, Y. H., Jung, T. G., Park, E. Y., Kang, G. W., Kim, K. A., & Lee, S. J. (2015). Biomechanical efficacy of a combined interspinous fusion system with a lumbar interbody fusion cage. *International Journal of Precision Engineering and Manufacturing, 16*(5), 997–1001.

19. Lim, J. W. (2018). Age-related stability for artificial disc fixators inserted into a lumbar vertebra: Finite element analysis. *International Journal of Precision Engineering and Manufacturing, 19*(2), 271–280.

20. Zheng, G., Nolte, L. P., & Ferguson, S. J. (2011). Scaled, patient-specific 3d vertebral model reconstruction based on 2d lateral fluoroscopy. *International Journal of Computer Assisted Radiology and Surgery, 6*(3), 351–366.

21. Goel, V. K., Mehta, A., Jangra, J., Faizan, A., Kiapour, A., Hoy, R. W., et al. (2007). Anatomic facet replacement system (afrs) restoration of lumbar segment mechanics to intact: A finite element study and in vitro cadaver investigation. *International Journal of Spine Surgery, 1*(1), 46–54.

22. Wu, H. C., & Ya, R. F. (1976). Mechanical behavior of the human annulus fibrosus. *Journal of Biomechanics, 9*(1), 1–7.

23. Kenedi, R. M. (1971). Strength of biological materials. *Journal of Anatomy, 108*(Pt 3), 582.

24. Renner, S. M., Natarajan, R. N., Patwardhan, A. G., Havey, R. M., Voronov, L. I., Guo, B. Y., et al. (2007). Novel model to analyze the effect of a large compressive follower pre-load on range of motions in a lumbar spine. *Journal of Biomechanics, 40*(6), 1326–1332.

25. Dreischarf, M., Zander, T., Shirazi-Adl, A., Puttlitz, C. M., Adam, C. J., Chen, C. S., et al. (2014). Comparison of eight published static finite element models of the intact lumbar spine: Predictive power of models improves when combined together. *Journal of Biomechanics, 47*(8), 1757–1766.

26. Kovacı, H., Yetim, A. F., & Çelik, A. (2018). Biomechanical analysis of spinal implants with different rod diameters under static and fatigue loads: An experimental study. *Biomedizinische Technik Biomedical Engineering, 64*(3), 339–346.

27. Gioia, G., Scotti, C., Mandelli, D., & Sala, G. (2011). Posterior spinal instrumentation: Biomechanical study on the role of rods on hardware response to axial load. *European Spine Journal, 20*, 3–7.

28. Brummund, M., Brailovski, V., Petit, Y., Facchinello, Y., & Mac-Thiong, J. M. (2017). Impact of spinal rod stiffness on porcine lumbar biomechanics: Finite element model validation and parametric study. *Proceedings of the Institution of Mechanical Engineers, Part H: Journal of Engineering in Medicine, 4*, 095441191773259.

29. Rohlmann, A., Burra, N. K., Zander, T., & Bergmann, G. (2007). Comparison of the effects of bilateral posterior dynamic and rigid fixation devices on the loads in the lumbar spine: A finite element analysis. *European Spine Journal, 18*(6), 1223–1231.

30. Chun, K., Yang, I., Kim, N., & Cho, D. (2015). Effect of device rigidity and physiological loading on spinal kinematics after

dynamic stabilization: An in-vitro biomechanical study. *Journal of Korean Neurosurgical Society*, *58*(5), 412–418.

31. Cheung, K., Karppinen, J., Chan, D., Ho, D., Song, Y., Sham, P., et al. (2009). Prevalence and pattern of lumbar magnetic resonance imaging changes in a population study of one thousand forty-three individuals. *Spine*, *34*(9), 934–940.

32. Ruberte, L. M., Natarajan, R. N., & Andersson, G. B. J. (2009). Influence of single-level lumbar degenerative disc disease on the behavior of the adjacent segments-a finite element model study. *Journal of Biomechanics*, *42*(3), 341–348.

33. Newell, R., Esfandiari, H., Anglin, C., Bernard, R., Street, J., & Hodgson, A. J. (2018). An intraoperative fluoroscopic method to accurately measure the post-implantation position of pedicle screws. *International Journal of Computer Assisted Radiology and Surgery*, *13*(8), 1257–1267.

34. Hooman, E., Robyn, N., Carolyn, A., John, S., & Hodgson, A. J. (2018). A deep learning framework for segmentation and pose estimation of pedicle screw implants based on c-arm fluoroscopy. *International Journal of Computer Assisted Radiology and Surgery*, *13*(8), 1269–1282.

35. Matsukawa, K., Yato, Y., Imabayashi, H., Hosogane, N., Abe, Y., Asazuma, T., et al. (2016). Biomechanical evaluation of fixation strength among different sizes of pedicle screws using the cortical bone trajectory: What is the ideal screw size for optimal fixation? *Acta Neurochirurgica*, *158*(3), 465–471.

36. Cho, D. Y., Liau, W. R., Lee, W. Y., Liu, J. T., Chiu, C. L., & Sheu, P. C. (2002). Preliminary experience using a polyetheretherketone (peek) cage in the treatment of cervical disc disease. *Neurosurgery*, *13*(6), 1343–1350.

37. Freudiger, S., Dubois, G., & Lorrain, M. (1999). Dynamic neutralisation of the lumbar spine confirmed on a new lumbar spine simulator in vitro. *Archives of Orthopaedic and Trauma Surgery*, *119*(3–4), 127–132.

38. Rohlmann, A., Burra, N. K., Zander, T., & Bergmann, G. (2007). Comparison of the effects of bilateral posterior dynamic and rigid fixation devices on the loads in the lumbar spine: A finite element analysis. *European Spine Journal*, *16*(8), 1223–1231.

39. Phillips, F. M., Reuben, J., & Wetzel, F. T. (2002). Intervertebral disc degeneration adjacent to a lumbar fusion: An experimental rabbit model. *Journal of Bone and Joint Surgery*, *84*(2), 289–294.

40. Chen, H. L., Guo, K. J., Yuan, F., & Ding, N. (2014). Effect of stress on intervertebral disc and facet joint of novel lumbar spine soft implant: Biomechanical analysis. *Biomedical Research*, *25*(2), 199–202.

41. Hsieh, Y. Y., Chen, C. H., Tsuang, F. Y., Wu, L. C., Lin, S. C., & Chiang, C. J. (2017). Removal of fixation construct could mitigate adjacent segment stress after lumbosacral fusion: A finite element analysis. *Clinical Biomechanics*, *43*, 115–120.

42. Lee, C. S., Hwang, C. J., Lee, S. W., Ahn, Y. J., Kim, Y. T., Lee, D. H., et al. (2009). Risk factors for adjacent segment disease after lumbar fusion. *European Spine Journal*, *18*(11), 1637.

43. Wittenberg, R. H., Shea, M., Edwards, W. T., Swartz, D. E., White, A. A., III, & Hayes, W. C. (1992). A biomechanical study of the fatigue characteristics of thoracolumbar fixator implants in a calf spine model. *Spine*, *17*(6), S121–S128.

44. Cunningham, B. W., Setter, J. C., Shono, Y., & Mcafee, P. C. (1993). Static and cyclical biomechanical analysis of pedicle screw spinal constructs. *Spine*, *18*(12), 1677–1688.

45. Newcomb, A. G., Baek, S., Kelly, B. P., & Crawford, N. R. (2016). Effect of screw position on load transfer in lumbar pedicle screws: A non-idealized finite element analysis. *Computer Methods in Biomechanics and Biomedical Engineering*, *20*(2), 182–192.

46. Chen, S. I., Lin, R. M., & Chang, C. H. (2003). Biomechanical investigation of pedicle screw–vertebrae complex: A finite element approach using bonded and contact interface conditions. *Medical Engineering & Physics*, *25*(4), 275–282.

47. Guo, L. X., Wang, Z. W., Zhang, Y. M., et al. (2009). Material property sensitivity analysis on resonant frequency characteristics of the human spine. *Journal of Applied Biomechanics*, *25*(1), 64–72.

Li-Xin Guo received his Ph.D. at Northeastern University, China. He was a Research Fellow at Nanyang Technological University, Singapore from 2002 to 2004. He was a Research Fellow at The Hong Kong Polytechnic University, Hong Kong, China in 2007, 2009, 2012. He has been a professor at Northeastern University since 2008. His research interests include Biomechanics, Mechanical CAE, Mechanical vibration and control and Vehicle dynamics.

Qing-Dong Wang received his Master degree from Northeastern University, China in 2017. He currently pursues a Ph.D. degree at the School of Mechanical Engineering and Automation, Northeastern University. His research interests include CAE analysis and Biomechanics.